ELSEVIER

Inorganica Chimica Acta 229 (1995) 105–112

Inorganica Chimica Acta

Reactions of monodentate tertiary phosphines with the dirhenium(II) alkyne complexes $[Re_2Cl_3(\mu\text{-dppm})_2(CO)(\eta^2\text{-RCCH})]X$ ($X = PF_6$ or O_3SCF_3) to form ylides ☆

Keng-Yu Shih, Robert M. Tylicki, Wengan Wu, Phillip E. Fanwick, R.A. Walton *

Department of Chemistry, Purdue University, 1393 Brown Building, West Lafayette, IN 47907-1393, USA

Received 3 May 1994; revised 17 June 1994

Abstract

The η^2-alkyne adducts $[Re_2Cl_3(\mu\text{-dppm})_2(CO)(\eta^2\text{-RCCH})]X$ (R = H, Pr^n, Bu^n or Ph; $X = PF_6$ or O_3SCF_3) have been reacted with monodentate tertiary phosphines PR_3 ($R_3 = Me_3$, Et_3, Me_2Ph or $MePh_2$) to afford in high yield (>60%) a new class of resonance stabilized ylides of composition $[Re_2Cl_3(\mu\text{-dppm})_2(CO)(C(R)CH(PR_3))]X$. These diamagnetic complexes have been characterized by IR, ^1H NMR and $^{31}P\{^1H\}$ NMR spectroscopies and cyclic voltammetry, and the structure of a representative example determined by single crystal X-ray crystallography. Crystal data for $[Re_2Cl_3(\mu\text{-dppm})_2(CO)(C(Pr^n)CH(PMe_2Ph))]SO_3CF_3 \cdot 0.83C_7H_8$ at 173 K: monoclinic space group *Pn* (No. 7), $a = 16.404(4)$, $b = 11.907(2)$, $c = 19.866(2)$ Å, $\beta = 110.58(1)°$, $V = 3632(2)$ Å^3, $Z = 2$. The structure was refined in full-matrix least-squares to $R = 0.052$ ($R_w = 0.068$) for 4156 data with $I > 3\sigma(I)$. This structure determination shows that the basic geometry present in the parent complexes $[Re_2Cl_3(\mu\text{-dppm})_2(CO)(\eta^2\text{-RCCH})]X$ is retained, the principal difference being the conversion of the η^2-alkyne ligand RCCH to the η^1-bound ylide $C(R)CH(PR_3)$. The Re–Re bond length of 2.311(1) Å signifies the retention of an Re≡Re bond.

Keywords: Rhenium complexes; Ylide complexes; Alkyne complexes; Crystal structures

1. Introduction

The multiply bonded A-frame-like dirhenium monocarbonyl complex $Re_2(\mu\text{-Cl})Cl_3(\mu\text{-dppm})_2(CO)$ (**1**; dppm = $Ph_2PCH_2PPh_2$) reacts with alkynes (RC≡CR′) in the presence of $TlPF_6$ to afford salts of the η^2-alkyne complexes $[Re_2Cl_3(\mu\text{-dppm})_2(CO)(\eta^2\text{-RCCR}')]^+$ (**2**) with retention of an Re–Re multiple bond [1]. These complexes, which can be isolated in the case of both internal and terminal alkynes [1], constitute the only cases to date in which an alkyne is bound in a dimetal complex that contains an electron-rich metal–metal triple bond ($\sigma^2\pi^4\delta^2\delta^{*2}$ electronic configuration) [2]. Since we had demonstrated previously that other mixed-ligand complexes derived from the synthon $Re_2Cl_4(\mu\text{-dppm})_2$ have the potential for exhibiting further coordinative unsaturation [3], we are examining the reactivity of complexes of type **2** towards various nucleophilic and electrophilic reagents. In this report we describe the reactions of several terminal alkyne-containing complexes of type **2** with monodentate tertiary phosphines which lead to a new class of resonance stabilized ylides, the first to be formed at quadruply or triply bonded dimetal centers based upon the $\sigma^2\pi^4\delta^a\delta^{*b}$ electronic configurations (where $a = 2$ when $b = 0$ or 2, and $a = 0$ when $b = 0$) [2].

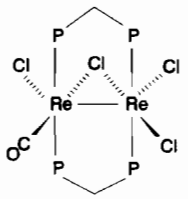

1

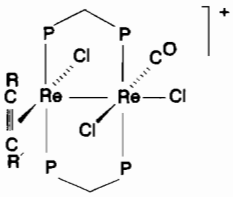

2

☆ This contribution is dedicated to Professor F. Albert Cotton on the occasion of his 65th birthday. One of the authors (R.A.W.) also takes this opportunity to recognize with great appreciation his almost thirty years of fruitful collaboration and close personal friendship with Professor Cotton. We wish this remarkable scientist many more years of creative and productive work.

* Corresponding author.

2. Experimental

2.1. Starting materials

The compounds $[Re_2Cl_3(\mu\text{-dppm})_2(CO)(\eta^2\text{-RCCH})]PF_6$ (R = H (**2a**), n-Pr (**2b**), n-Bu (**2c**), Ph (**2d**)) were

0020-1693/95/$09.50 © 1995 Elsevier Science S.A. All rights reserved
SSDI 0020-1693(94)04234-M

prepared according to the literature procedures [1]. Ethyne, both unlabeled and ^{13}C labeled (99.1%), was obtained from Matheson Gas Products. All other alkynes were obtained from the Aldrich Chemical Co. The phosphines PR_3 ($R_3 = Me_3$, Et_3, $MePh_2$, Me_2Ph) were purchased from Strem Chemicals and used without further purification. Solvents were obtained from commercial sources.

2.2. Reaction procedures

All reactions were performed under an atmosphere of dry nitrogen. Solvents other than THF were deoxygenated by purging with nitrogen gas prior to use. The tetrahydrofuran solvent was freshly distilled from sodium under nitrogen prior to use.

2.2.1. Synthesis of $[Re_2Cl_3(\mu\text{-dppm})_2(CO)(\eta^2\text{-}RCCR')]SO_3CF_3$ ($R = Pr^n$, $R' = H$ (2e); $R = Me$, $R' = Et$ (2f))

A procedure similar to that used to prepare complexes **2a–2d** was employed to synthesize **2e** and **2f** through the use of the $TlSO_3CF_3$ [4] in place of $TlPF_6$. Yields: **2e**, 87%; **2f**, 81%. IR spectra (ν(CO), cm^{-1}): **2e**, 1942(s); **2f**, 1938(s).

2.2.2. Reactions of $[Re_2Cl_3(\mu\text{-dppm})_2(CO)(\eta^2\text{-}RCCH)]X$ with tertiary phosphines PR_3. Synthesis of $[Re_2Cl_3(\mu\text{-dppm})_2(CO)(C(R)CH(PR_3))]X$

(i) $R = H$, $PR_3 = PMe_3$, $X = PF_6$ (3a). A suspension of **2a** (0.050 g, 0.035 mmol) in THF (6 ml) was treated with PMe_3 (0.020 ml). The green complex $[Re_2Cl_3(dppm)_2(CO)(CHCH(PMe_3))]PF_6$ (**3a**) began to precipitate within 5 min and was filtered off after 3 h. The product was washed with diethyl ether (3×5 ml) and dried under vacuum. Yield 0.032 g (61%). ^1H NMR spectrum (δ in CD_2Cl_2): 7.0–7.8 (m, 42H), 5.44 (m, 2H), 5.14 (m, 2H), 1.41 (d, 9H). $^{31}P\{^1H\}$ NMR spectrum (δ in CD_2Cl_2): 6.70 (m), 1.80 (m), −3.98 (m), −143.9 (h).

The ^{13}C labeled derivative, $[Re_2Cl_3(dppm)_2(CO)(^{13}CH^{13}CH(PMe_3))]PF_6$, was synthesized through a procedure similar to that described above by the use of the ^{13}C-labeled parent complex $[Re_2Cl_3(dppm)_2(CO)(\eta^2\text{-}H^{13}C^{13}CH)]PF_6$. ^1H NMR spectrum (δ in CD_2Cl_2): 7.1–7.8 (m, 42H), 5.45 (m, 2H), 5.09 (m, 2H), 1.33 (d, 9H).

(ii) $R = H$, $PR_3 = PEt_3$, $X = PF_6$ (3b). A mixture of **2a** (0.045 g, 0.032 mmol) and PEt_3 (0.050 ml) was reacted in THF (5 ml) using a procedure similar to that described in Section 2.2.2.(i). A reaction time of 15 h was used and the product **3b** was recrystallized from dichloromethane/diethyl ether. Yield 0.032 g (66%). ^1H NMR spectrum (δ in CD_2Cl_2): 7.05–7.75 (m, 40H), 5.50 (m, 2H), 5.00 (m, 2H), 1.87 (m, 6H), 1.00 (m, 9H). $^{31}P\{^1H\}$ NMR spectrum (δ in CD_2Cl_2): 18.24 (s), 2.05 (m), −4.49 (m), −144.0 (h).

(iii) $R = H$, $PR_3 = PMePh_2$, $X = PF_6$ (3c). A reaction time of 12 h was used to synthesize the complex $[Re_2Cl_3(dppm)_2(CO)(CHCH(PMePh_2))]PF_6$ (**3c**) from the reaction of **2a** with $PMePh_2$. The workup was very similar to that described in Section 2.2.2.(i) except that the resulting reaction mixture was treated with an excess of diethyl ether to induce precipitation of the product. Yield 82%. *Anal.* Calc. for $C_{66}H_{59}Cl_3OP_5Re_2$: C, 49.06; H, 3.68. Found: C, 49.44; H, 3.78%. ^1H NMR spectrum (δ in $CDCl_3$): 7.0–7.8 (m, 52H), 5.67 (m, 2H), 5.01 (m, 2H), 1.93 (m, 3H). $^{31}P\{^1H\}$ NMR spectrum (δ in $CDCl_3$): 7.40 (s), −0.34 (m), −6.42 (m), −143.5 (h).

(iv) $R = Pr^n$, $PR_3 = PMe_3$, $X = PF_6$ (3d). A suspension of **2b** (0.050 g, 0.033 mmol) in THF (5 ml) was treated with PMe_3 (0.070 ml). The resulting mixture was heated to reflux for 1 h and the green precipitate of $[Re_2Cl_3(dppm)_2(CO)(C(n\text{-}Pr)CH(PMe_3))]PF_6$ (**3d**) was filtered off after the reaction mixture had cooled to room temperature. The solid was washed with diethyl ether (3×5 ml) and dried under vacuum. Yield 0.035 g (68%). *Anal.* Calc. for $C_{59}H_{61}Cl_3F_6OP_6Re_2$: C, 44.58; H, 3.64. Found: C, 45.28; H, 3.94%. ^1H NMR spectrum (δ in CD_2Cl_2): 7.15–7.95 (m, 40H), 6.89 (d, 1H, ^2J(P–H) = 25.5 Hz), 5.64 (m, 4H), 1.83 (d, 9H, ^2J(P–H) = 12.9 Hz), 0.21 (m, 2H), −0.04 (t, 3H), −0.77 (m, 2H). $^{31}P\{^1H\}$ NMR spectrum (δ in CD_2Cl_2): −1.90 (s), −5.40 (m), −18.08 (m), −143.9 (h).

(v) $R = Pr^n$, $PR_3 = PEt_3$, $X = PF_6$ (3e). A procedure similar to that described in Section 2.2.2.(iv) was used to convert **2b** into $[Re_2Cl_3(dppm)_2(CO)(C(n\text{-}Pr)CH(PEt_3))]PF_6$ (**3e**) but with the use of a longer reaction time (18 h). Yield 62%. ^1H NMR spectrum (δ in CD_2Cl_2): 7.10–7.95 (m, 40H), 6.71 (d, 1H, ^2J(P–H) = 23.4 Hz), 5.65 (m, 4H), 2.08 (m, 6H), 1.30 (m, 9H), −0.07 (t, 3H), −0.32 (m, br, 4H). $^{31}P\{^1H\}$ NMR spectrum (δ in CD_2Cl_2): 12.22 (s), −5.52 (m), −18.32 (m), −144.0 (h).

(vi) $R = Bu^n$, $PR_3 = PMe_3$, $X = PF_6$ (3f). The reaction of **2c** with PMe_3 through the use of a procedure similar to that described in Section 2.2.2.(iv) afforded the title complex **3f**. Yield 70%. *Anal.* Calc. for $C_{60}H_{63}Cl_3F_6OP_5Re_2$: C, 46.56; H, 4.10. Found: C, 45.59; H, 4.28%. ^1H NMR spectrum (δ in CD_2Cl_2): 7.15–7.95 (m, 40H), 6.89 (d, 1H, ^2J(P–H) = 25.6 Hz), 5.65 (m, 4H), 1.86 (d, 9H, ^2J(P–H) = 12.9 Hz), 0.26 (m, 2H), 0.14 (t, 3H), 0.079 (m, 2H), −0.59 (m, 2H). $^{31}P\{^1H\}$ NMR spectrum (δ in CD_2Cl_2): −2.20 (s), −5.33 (m), −18.45 (m), −143.9 (h).

(vii) $R = Ph$, $PR_3 = PMe_3$, $X = PF_6$ (3g). The reaction of **2d** with PMe_3 was carried out for 20 h to produce $[Re_2Cl_3(dppm)_2(CO)(C(Ph)CH(PMe_3))]PF_6$ (**3g**) as a green insoluble product. Yield 66%. *Anal.* Calc. for $C_{62}H_{59}Cl_3F_6OP_5Re_2$: C, 47.50; H, 3.79. Found: C, 46.25; H, 4.05%. ^1H NMR spectrum (δ in CD_2Cl_2): 7.00–7.85 (m, 41H), 6.89 (d, 1H, ^2J(P–H) = 30 Hz), 6.48 (t, 2H),

5.67 (m, 2H), 5.56 (m, 2H), 5.15 (d, 2H), 2.00 (d, 9H). $^{31}P\{^1H\}$ NMR spectrum (δ in CD_2Cl_2): 1.10 (s), −4.10 (m), −7.80 (m), −143.5 (h).

(viii) $R=Pr^n$, $PR_3=PMe_3$, $X=O_3SCF_3$ (3h). A suspension of **2e** (0.174 g, 0.117 mmol) in THF (15 ml) was treated with PMe_3 (0.10 ml, 1.0 mmol). The resulting mixture was heated to reflux for 1.5 h. It was then cooled to room temperature and the green precipitate of $[Re_2Cl_3(dppm)_2(CO)(C(n\text{-}Pr)CH(PMe_3))]SO_3CF_3$ (**3h**) was filtered off, washed with diethyl ether and dried under vacuum. Yield 0.144 g (78%). *Anal.* Calc. for $C_{60}H_{61}Cl_3F_3O_4P_5Re_2S$: C, 45.93; H, 3.92. Found: C, 45.20; H, 4.13%. ^1H NMR spectrum (δ in CD_2Cl_2): 7.10–7.95 (m, 40H), 6.90 (d, 1H, ^2J(P–H) = 25.4 Hz), 5.67 (m, 4H), 1.90 (d, 9H, ^2J(P–H) = 13.1 Hz), 0.26 (m, 2H), −0.08 (t, 3H, ^2J(H–H) = 6.7 Hz), −0.85 (m, 2H). $^{31}P\{^1H\}$ NMR spectrum (δ in $(CD_3)_2CO$): −1.89 (s), −5.00 (m), −16.84 (m); (δ in CD_2Cl_2): −1.58 (s), −5.20 (m), −18.10 (m).

(ix) $R=Pr^n$, $PR_3=PMe_2Ph$, $X=O_3SCF_3$ (3i). This complex was prepared from **2e** by the use of a procedure similar to that described in Section 2.2.2.(viii) but with a reaction time of 24 h. Yield 87%. *Anal.* Calc. for $C_{65}H_{63}Cl_3F_3O_4P_5Re_2S$: C, 47.32; H, 3.85. Found: C, 47.69; H, 3.91%. ^1H NMR spectrum (δ in $CDCl_3$): 7.03–7.95 (m, 46H), 5.76 (m, 4H), 2.18 (d, 6H, ^2J(P–H) = 13.0 Hz), 0.30 (m, 2H), −0.20 (t, 3H, ^2J(H–H) = 6.7 Hz), −1.13 (m, 2H). $^{31}P\{^1H\}$ NMR spectrum (δ in $(CD_3)_2CO$): −1.91 (s), −4.96 (m), −16.80 (m).

2.2.3. Reaction of $[Re_2Cl_3(dppm)_2(CO)(\eta^2\text{-Me-CCEt})]SO_3CF_3$ (2f) with PMe_2Ph

A suspension of **2f** (0.100 g, 0.067 mmol) in THF (10 ml) was treated with PMe_2Ph (0.050 ml) and then was heated to reflux for 24 h. A blue–green solution, along with a very small amount of white precipitate, formed. This resulting mixture was filtered, and the volume of the blue–green filtrate was reduced to ~2 ml on a rotary evaporator and then treated with an excess of diethyl ether (up to 50 ml). The oily precipitate was characterized by IR spectroscopy and cyclic voltammetry which showed it to be a mixture that did not contain an ylide complex.

2.3. X-ray crystallography

Single crystals of complex **3i** suitable for diffraction analysis were grown by the slow evaporation of the solvents from a solution of **3i** in 1,2-dichloroethane/toluene (2/1) at 25 °C. A needle crystal of **3i** having approximate dimensions of 0.40×0.25×0.10 mm was mounted on a glass fiber and cooled immediately to 173±1 K. The data collection was performed on an Enraf-Nonius CAD4 computer controlled diffractometer with graphite-monochromatized Mo Kα radiation at 173±1 K. The cell contents were based on 25 reflections obtained in the range of $16<\theta<18°$. Three standard reflections were measured after every 5000 s of beam time during data collection and there were no systematic variations in intensity. Calculations were performed on a microVAX II computer using the Enraf-Nonius structure determination package. Lorentz and polarization corrections were applied to the data set. An empirical absorption correction [5] was also applied, but no correction for extinction was made.

Complex **3i** crystallized in the monoclinic crystal system. On the basis of systematic absences observed on the data set, the crystal of **3i** was concluded to belong to space group *Pn* or *P2/n*. However, with $Z=2$, complex **3i** would have to possess either a two-fold axis or a center of symmetry in order to crystallize in *P2/n*. The acentric space group *Pn* was therefore assumed, and subsequently confirmed by the successful solution and refinement of the structure. The structure was solved by the use of the Patterson heavy atom method which revealed the positions of the Re atoms. The remaining non-hydrogen atoms were located in succeeding difference Fourier syntheses. Due to the limited data, only atoms heavier than fluorine were refined anisotropically and all other atoms refined with isotropic thermal parameters. Corrections for anomalous scattering were applied to the anisotropically refined atoms [6]. The hydrogen atoms were not included in the calculations. The structure was refined in full-matrix least-squares where the function minimized was $\Sigma w(|F_o|-|F_c|)^2$, where w is the weighting factor defined as $w=1/\sigma^2(F_o)$. In the final stages of the refinement of **3i** a disordered molecule of toluene, originating from the crystallization solvent mixture, was found. All six of the ring carbon atoms were located and satisfactorily refined with isotropic thermal parameters and a multiplicity of 0.83. The final residuals for **3i** were $R=0.052$ ($R_w=0.068$) and $GOF=1.854$; for the other enantiomorph $R=0.053$ ($R_w=0.068$) and $GOF=1.867$. The highest peak in the final difference Fourier was 2.5 e Å^{-3}.

The basic crystallographic parameters for complex **3i** are listed in Table 1. Positional parameters and their errors for the non-hydrogen atoms of **3i**, except the phenyl group atoms of the dppm ligands and the atoms of the toluene solvent molecule, are listed in Table 2. Important intramolecular bond distances and angles are given in Table 3. See also Section 5.

2.4. Physical measurements

IR spectra were recorded as Nujol mulls between KBr disks on a Perkin-Elmer 1800 FT-IR spectrometer. Electrochemical measurements were carried out on dichloromethane solutions that contained 0.1 M tetra-n-butylammonium hexafluorophosphate (TBAH) as

Table 1
Crystallographic data and data collection parameters for $[Re_2Cl_3(\mu\text{-dppm})_2(CO)(C(Pr^n)CH(PMe_2Ph))]SO_3CF_3 \cdot 0.83C_7H_8$ (**3i**)

Formula	$Re_2Cl_3SP_5F_3O_4C_{70.81}H_{69.64}$
Formula weight	1707.39
Space group	*Pn* (No. 7)
a (Å)	16.404(4)
b (Å)	11.907(2)
c (Å)	19.866(2)
β (°)	110.58(1)
V (Å^3)	3632(2)
Z	2
D_c (g cm^{-3})	1.561
Crystal dimensions (mm)	0.40×0.25×0.10
Temperature (K)	173
Radiation, wavelength (Å)	Mo Kα, 0.71073
Monochromator	graphite
Linear absorption coefficient (cm^{-1})	36.68
Absorption correction applied	empirical [a]
Transmission factors: min., max.	0.70, 1.00
Diffractometer	Enraf-Nonius CAD4
Scan method	ω–2θ
h, *k*, *l* Limits	−16 to 17, 0 to 12, −21 to 0
2θ Range (°)	6.02–45.00
Scan width (°)	1.09+1.31 tan (θ)
Take-off angle (°)	3.00
Program used	Enraf-Nonius MolEN
F(000)	1694.0
p-Factor used in weighting	0.040
Data collected	5166
Unique data	5002
Agreement factor (on *I*)	0.056
Data with $I>3.0\sigma(I)$	4156
No. variables	423
Largest shift/e.s.d. in final cycle	0.05
R [b]	0.052
R_w [c]	0.068
GOF [d]	1.854

[a] See Ref. [5].
[b] $R=\Sigma||F_o|-|F_c||/\Sigma|F_o|$.
[c] $R_w=[\Sigma w(|F_o|-|F_c|)^2/\Sigma w|F_o|^2]^{1/2}$; $w=1/\sigma^2(F_o)$.
[d] Goodness of fit $=[\Sigma w(|F_o|-|F_c|)^2/(N_{obs}-N_{param})]^{1/2}$.

Table 2
Positional parameters for selected non-hydrogen atoms in **3i** and their e.s.d.s [a]

Atom	*x*	*y*	*z*	*B* (Å^2)
Re(1)	0	0.19744(7)	0	1.25(2)
Re(2)	−0.03359(7)	0.35239(7)	−0.07486(6)	1.26(2)
Cl(11)	0.0245(3)	0.0046(5)	0.0581(3)	2.0(1)
Cl(12)	0.0772(3)	0.2684(5)	0.1186(3)	1.8(1)
Cl(21)	−0.0553(4)	0.3171(5)	−0.2018(2)	2.5(1)
P(11)	−0.1313(4)	0.2041(5)	0.0290(3)	1.7(1)
P(12)	0.1461(4)	0.1574(5)	−0.0101(3)	1.9(1)
P(21)	−0.1866(4)	0.3423(5)	−0.1010(3)	1.6(1)
P(22)	0.1178(4)	0.3869(5)	−0.0803(3)	1.9(1)
P(23)	−0.0073(4)	0.6186(5)	0.1116(3)	1.9(1)
O(1)	−0.0714(9)	0.051(1)	−0.1393(8)	1.7(3) *
C(1)	−0.046(1)	0.110(2)	−0.083(1)	1.0(4) *
C(1B)	−0.197(1)	0.324(2)	−0.014(1)	1.6(4) *
C(21)	−0.029(1)	0.488(2)	−0.011(1)	0.8(3) *
C(22)	−0.024(1)	0.501(2)	0.058(1)	1.9(4) *
C(2B)	0.157(1)	0.245(2)	−0.082(1)	1.9(4) *
C(211)	−0.026(2)	0.587(2)	−0.060(1)	3.1(5) *
C(212)	−0.090(1)	0.687(2)	−0.065(1)	1.8(4) *
C(213)	−0.079(2)	0.784(3)	−0.117(2)	4.2(6) *
C(231)	−0.104(1)	0.689(2)	0.109(1)	1.8(4) *
C(232)	−0.183(2)	0.639(2)	0.079(1)	2.6(5) *
C(233)	−0.261(2)	0.684(3)	0.082(2)	4.0(6) *
C(234)	−0.256(2)	0.789(2)	0.111(2)	3.7(6) *
C(235)	−0.175(2)	0.852(3)	0.139(2)	4.0(6) *
C(236)	−0.101(2)	0.794(2)	0.135(1)	3.1(5) *
C(237)	0.039(2)	0.564(2)	0.203(1)	2.9(5) *
C(238)	0.072(2)	0.718(2)	0.102(1)	2.8(5) *
S(100)	0.5394(5)	0.401(1)	0.9919(5)	6.7(3)
F(101)	0.499(2)	0.405(3)	0.856(1)	12(1)
F(102)	0.485(3)	0.241(4)	0.917(2)	24(2)
F(103)	0.394(1)	0.417(4)	0.887(2)	16(1)
O(101)	0.621(2)	0.383(2)	1.005(1)	6.5(6) *
O(102)	0.496(2)	0.379(2)	1.039(1)	5.9(6) *
O(103)	0.527(3)	0.547(4)	0.966(2)	13(1) *
C(104)	0.470(4)	0.382(5)	0.907(3)	11(2) *

[a] Anisotropically refined atoms are given in the form of the isotropic equivalent thermal parameter defined as: $(4/3)[a^2\beta(1,1)+b^2\beta(2,2)+c^2\beta(3,3)+ab(\cos\gamma)\beta(1,2)+ac(\cos\beta)\beta(1,3)+bc(\cos\alpha)\beta(2,3)]$. For data for the phenyl atoms of the dppm ligands and the carbon atoms of the toluene molecule of crystallization, see Section 5. An asterisk denotes a value for an isotropically refined atom.

supporting electrolyte. $E_{1/2}$ values, determined as $(E_{p,a}+E_{p,c})/2$, were referenced to the silver/silver chloride (Ag/AgCl) electrode at 25 °C and are uncorrected for junction potentials. Under our experimental conditions $E_{1/2}=0.47$ V versus Ag/AgCl for the ferrocenium/ferrocene couple. Voltammetric experiments were performed with a BAS Inc. model CV-27 instrument in conjunction with a BAS model RXY recorder. NMR spectra were recorded on CD_2Cl_2, $CDCl_3$ or $(CD_3)_2CO$ solutions of the complexes. ^{1}H NMR spectra were obtained with the use of a Varian Gemini-200 or a GE QE-300 spectrometer. A Varian XL-200 spectrometer operated at 80.98 MHz or a GE QE-300 spectrometer equipped with a multinuclear Quad prob operated at 121.5 MHz with 85% H_3PO_4 as an external standard was used to obtain the $^{31}P\{^1H\}$ NMR spectra. $^{13}C\{^1H\}$ NMR spectra were recorded on a GE QE-300 spectrometer operated at 75.61 MHz. Elemental microanalyses were performed by Dr H.D. Lee of the Purdue University Microanalytical Laboratory. Representative microanalytical data are given in Section 2.2.

3. Results and discussion

The reactions of the η^2-alkyne complexes $[Re_2Cl_3(\mu\text{-dppm})_2(CO)(\eta^2\text{-RCCH})]X$ (**2**) with monodentate tertiary phosphines proceed as shown in Scheme 1 to afford the dirhenium ylide complexes **3** in quite high yield (>60%). The use of the ^{13}C-labeled ethyne analogue of **2a** gave the corresponding ^{13}C-labeled ylide

Table 3
Some important bond distances (Å) and bond angles (°) for **3i** [a]

Bond distances			
Re(1)–Re(2)	2.311(1)	P(23)–C(22)	1.72(2)
Re(1)–Cl(11)	2.538(6)	P(23)–C(231)	1.78(3)
Re(1)–Cl(12)	2.402(6)	P(23)–C(237)	1.83(3)
Re(1)–P(11)	2.418(7)	P(23)–C(238)	1.82(3)
Re(1)–P(12)	2.521(7)	O(1)–C(1)	1.26(3)
Re(1)–C(1)	1.87(2)	C(21)–C(22)	1.37(3)
Re(2)–Cl(21)	2.456(6)	C(21)–C(211)	1.54(3)
Re(2)–P(21)	2.381(7)	C(211)–C(212)	1.56(4)
Re(2)–P(22)	2.556(7)	C(212)–C(213)	1.60(4)
Re(2)–C(21)	2.03(2)		
Bond angles			
Re(2)–Re(1)–Cl(11)	168.1(1)	Cl(21)–Re(2)–P(21)	90.4(2)
Re(2)–Re(1)–P(12)	105.9(1)	P(21)–Re(2)–C(21)	88.9(6)
Re(2)–Re(1)–P(11)	95.5(2)	P(22)–Re(2)–C(21)	94.3(6)
Re(2)–Re(1)–P(12)	96.8(2)	C(22)–P(23)–C(231)	115(1)
Re(2)–Re(1)–C(1)	87.0(7)	C(22)–P(23)–C(237)	104(1)
Cl(11)–Re(1)–Cl(12)	85.8(2)	C(22)–P(23)–C(238)	115(1)
Cl(11)–Re(1)–P(11)	86.2(2)	C(231)–P(23)–C(237)	105(1)
Cl(11)–Re(1)–P(12)	82.1(2)	C(231)–P(23)–C(238)	111(1)
Cl(11)–Re(1)–C(1)	81.1(7)	C(237)–P(23)–C(238)	106(1)
Cl(12)–Re(1)–P(11)	87.8(2)	Re(1)–C(1)–O(1)	175(2)
Cl(12)–Re(1)–P(12)	87.5(2)	Re(2)–C(21)–C(22)	134(2)
Cl(12)–Re(1)–C(1)	166.0(7)	Re(2)–C(21)–C(211)	103(2)
P(11)–Re(1)–P(12)	167.6(2)	C(22)–C(21)–C(211)	123(2)
P(11)–Re(1)–C(1)	96.3(7)	Cl(21)–Re(2)–P(22)	77.1(2)
P(12)–Re(1)–C(1)	85.8(7)	Cl(21)–Re(2)–C(21)	137.2(6)
Re(1)–Re(2)–Cl(21)	116.1(2)	P(21)–Re(2)–P(22)	164.6(2)
Re(1)–Re(2)–P(21)	95.4(2)	P(23)–C(22)–C(21)	131(2)
Re(1)–Re(2)–P(22)	98.1(2)	C(21)–C(211)–C(212)	118(2)
Re(1)–Re(2)–C(21)	106.6(6)	C(211)–C(212)–C(213)	112(2)

[a] Numbers in parentheses are e.s.d.s in the least significant digits.

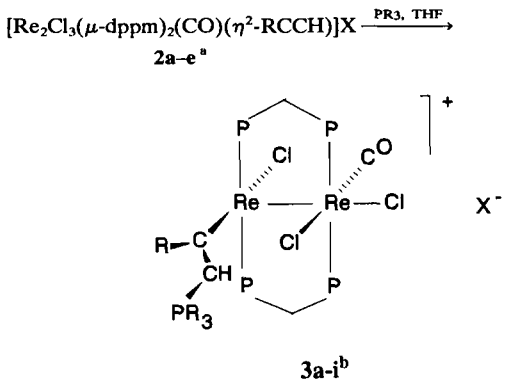

[a] R = H, X = PF_6 (**2a**); R = Pr^n, X = PF_6 (**2b**); R = Bu^n, X = PF_6 (**2c**); R = Ph, X = PF_6 (**2d**); R = Pr^n, X = SO_3CF_3 (**2e**).
[b] R = H, PR_3 = PMe_3, X = PF_6 (**3a**); R = H, PR_3 = PEt_3, X = PF_6 (**3b**); R = H, PR_3 = $PMePh_2$, X = PF_6 (**3c**); R = Pr^n, PR_3 = PMe_3, X = PF_6 (**3d**); R = Pr^n, PR_3 = PEt_3, X = PF_6 (**3e**); R = Bu^n, PR_3 = PMe_3, X = PF_6 (**3f**); R = Ph, PR_3 = PMe_3, X = PF_6 (**3g**); R = Pr^n, PR_3 = PMe_3, X = O_3SCF_3 (**3h**); R = Pr^n, PR_3 = PMe_2Ph, X = O_3SCF_3 (**3i**).

Scheme 1. Reactions of **2** with monodentate tertiary phosphines to produce the ylide complexes **3**.

complex. These green, diamagnetic complexes are formally the products of the nucleophilic attack of the phosphine on the C–H carbon of the terminal alkyne. The reactions of **2** with PR_3 were carried out for periods of up to 24 h; longer times did not seem to adversely affect the product yields.

The reactions proceed equally well with a variety of terminal alkynes (R = H, Pr^n, Bu^n or Ph) and with the use of the phosphines PMe_3, PMe_2Ph, $PMePh_2$ or PEt_3. The failure of internal alkyne complexes of type **2** to react in this same fashion with PR_3 ligands was shown by a study of the reaction between $[Re_2Cl_3(\mu\text{-dppm})_2(CO)(\eta^2\text{-MeCCEt})]SO_3CF_3$ (**2f**) and PMe_2Ph. In this case we find no evidence for ylide formation. Alkyne displacement by the PMe_2Ph ligand does not apparently occur since we find no IR spectral evidence for the formation of $[Re_2Cl_3(\mu\text{-dppm})_2(\mu\text{-CO})(PMe_2Ph)_2]^+$, the most likely product of such a reaction course [7].

The green, diamagnetic complexes **3** display a single intense ν(CO) mode in their IR spectra between 1930 and 1970 cm^{-1} (Table 4); this frequency range is very similar to that observed for the ν(CO) mode of the precursor complexes **2**. The ν(P–F) mode of the $[PF_6]^-$

Table 4
Selected electrochemical and IR spectral data for ylide complexes of the type $[Re_2Cl_3(\mu\text{-dppm})_2(CO)(C(R)CH(PR_3))]X$ (3)

Complex	R	PR_3	X	CV half-wave potentials [a] (V)		IR spectra [c] (cm^{-1})
				$E_{1/2}$(ox) [b]	$E_{p,c}$	ν(CO)
3a	H	PMe_3	PF_6	+0.89(60)	−1.00 [d]	1936
3b	H	PEt_3	PF_6	+0.93(60)	−0.99 [d]	1937
3c	H	$PMePh_2$	PF_6	+0.97(60)	−1.02 [d]	1966
3d	Pr^n	PMe_3	PF_6	+0.90(70)	−1.13 [e]	1963
3e	Pr^n	PEt_3	PF_6	+0.92(60)	−1.05	1965
3f	Bu^n	PMe_3	PF_6	+0.91(60)	−1.08 [e]	1968
3g	Ph	PMe_3	PF_6	+0.91(60)	−1.16	1944
3h	Pr^n	PMe_3	O_3SCF_3	+0.87(70)	−1.13	1964
3i	Pr^n	PMe_2Ph	O_3SCF_3	+0.92(75)	−1.13 [e]	1962

[a] Measured on 0.1 M TBAH–CH_2Cl_2 solutions and referenced to the Ag/AgCl electrode with a scan rate (ν) of 200 mV s^{-1} at a Pt-bead electrode. Under our experimental conditions $E_{1/2}$ = +0.47 V vs. Ag/AgCl for the ferrocenium/ferrocene couple.
[b] ΔE_p ($E_{p,a} - E_{p,c}$) values are given in parentheses.
[c] Recorded as nujol mulls.
[d] This process overlaps a second, reversible process at more negative potentials ($E_{1/2}$(red) ~ −1.05 V); also, a product wave is found at $E_{p,a}$ ~ −0.4 V.
[e] A second irreversible reduction process is present at $E_{p,c}$ ~ −1.3 V.

anion is found at ~840 cm^{-1} in the spectra of **3a–3g**; for the $[CF_3SO_3]^-$ salts **3h** and **3i**, a characteristic anion vibrational mode is observed at ~1260 cm^{-1}. The 1:1 electrolyte behavior of these complexes was confirmed by conductivity measurements [8] on acetone solutions of **3c**, **3f** and **3g** (~1×10^{-3} M) for which Λ_m = 108, 106 and 118 Ω^{-1} cm^2 mol^{-1}, respectively.

The cyclic voltammetric (CV) properties of **3** are very similar (Table 4). Solutions in 0.1 M TBAH–CH_2Cl_2 show a reversible one-electron oxidation close to +0.9 V versus Ag/AgCl, and an irreversible reduction between −1.0 and −1.2 V. In some instances, processes that are attributable to the chemical products of this irreversible reduction can be identified (Table 4). The similarities of the IR spectra and CV properties of all the complexes of type **3** imply that they are structurally very similar.

The structural identity of a member of this series of complexes, **3i**, was established by a single crystal X-ray structure analysis. An ORTEP representation of the structure of the dirhenium cation that is present in the crystals of $[Re_2Cl_3(\mu\text{-dppm})_2(CO)(C(Pr^n)\text{-}CH(PMe_3))]O_3SCF_3\cdot0.83C_7H_8$ is shown in Fig. 1. The crystallographic data and important structural parameters are given in Tables 1–3. The structure of the dirhenium cation of **3i** closely resembles that of the parent precursor complex **2** with the exception that the terminally bound η^2-alkyne ligand (RCCH) has been converted to an η^1-bound C(R)CH(PR_3) ylide ligand. With the exception of this ligand change, the structural parameters for complexes of types **2** and **3** are generally quite similar as seen from a comparison of the crystal structures of $[Re_2Cl_3(\mu\text{-dppm})_2(CO)(\eta^2\text{-MeCCEt})]PF_6$ [1] and **3i**. A noticeable feature in the structure of **3i** is the disparity within the sets of *trans* Re–P bond

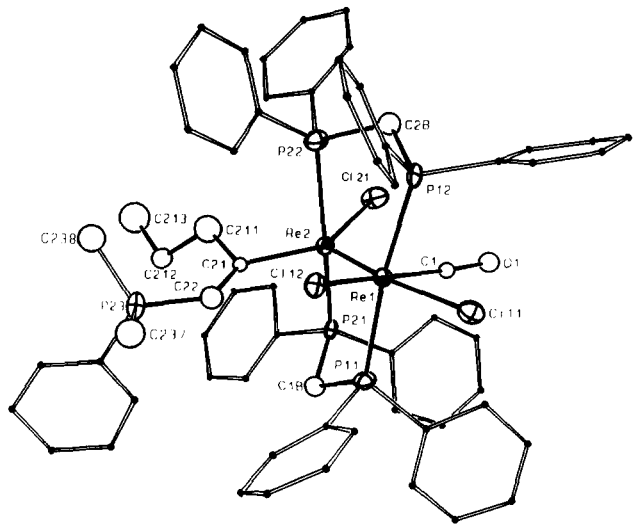

Fig. 1. ORTEP representation of the structure of the dirhenium cation $[Re_2Cl_3(\mu\text{-dppm})_2(CO)(C(Pr^n)CH(PMe_2Ph))]^+$ as present in complex **3i**, showing the numbering of the important atoms. The thermal ellipsoids are drawn at the 50% probability level except for the carbon atoms of the phenyl rings which are of arbitrary size. A full atomic numbering scheme is available, see Section 5.

lengths (≥0.1 Å); the reason for this is unclear, although in both structures these pairs of *trans* Re–P bonds average ~2.47 Å. The Re–Re bond length for **3i** of 2.311(1) Å (Table 3) is a little shorter (by ~0.03 Å) than that present in the structurally characterized η^2-alkyne complex [1], but is similar to the Re≡Re bond distance in other dirhenium(II) complexes [2]. A partial staggered geometry in **3i** is reflected by the torsional angles Cl(12)–Re(1)–Re(2)–C(21), P(11)–Re(1)–Re(2)–P(21), P(12)–Re(1)–Re(2)–P(22) and C(1)–Re(1)–Re(2)–Cl(21) which are 21.4(6), 22.7(2), 13.9(2) and 19.7(7)°, respectively.

While ylides have been prepared previously by phosphine attack on coordinated alkynes [1], the most relevant comparison of the present results is to the recent study on mononuclear rhenium complexes by Hoffman et al. [10]. The structure of the Re[C(Pr^n)CH(PMe$_2$Ph)] moiety in **3i** resembles that of the ylide structural units that are present in the mononuclear complexes Re(O)(CH$_2$SiMe$_3$)$_3$(CHCH(PMe$_3$)) and [Re(O)Me$_2$-(CHCH(PMe$_2$)Ph)$_2$]Cl [10]. The Re(2)–C(21) bond length (2.03(2) Å) signifies the presence of some degree of partial Re–C multiple bond character [10,11], while the carbon–carbon distance C(21)–C(22) of 1.37(3) Å, which is much shorter than the conjoined distance C(21)–C(211) (1.54(3) Å), accords with an olefinic-like linkage. The P–CHC(R)Re distance of 1.72(2) Å is similar to the comparable P–C distances that are present in the oxorhenium–ylide complexes reported by Hoffman et al. [10]. These results are best interpreted in terms of the resonance structures **Ia** and **Ib** being the dominant contributors to the overall structure.

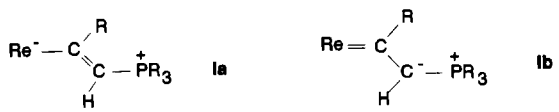

The ^{1}H and ^{31}P{^{1}H} NMR spectral data for these complexes (recorded in CD$_2$Cl$_2$, CDCl$_3$ or (CD$_3$)$_2$CO) are listed in Section 2. The ^{1}H NMR spectra accord with the structural formulation of these complexes as ylides. The unique Re[C(R)C*H*(PR$_3$)] hydrogen atom of the ylide ligand is observed as a doublet between δ +6.7 and +6.9 (^2J(P–H) in the range 23–30 Hz) in the spectra of **3d–3h**. The spectrum of **3i** does not show this feature since it is apparently shifted downfield slightly and becomes obscured by the complex pattern of phenyl resonances which are located between δ +7.0 and 8.0. The ^{1}H NMR spectra of complexes **3a–3c**, which are derived from η^2-ethyne precursors, are more problematic. In addition to the resonances that are listed in Section 2, the spectrum of the PEt$_3$ derivative **3b** shows two very broad and weak features at δ +11.4 and +3.05 in CD$_2$Cl$_2$ (an almost identical spectrum is observed in CDCl$_3$). These peaks could be due to the ReC*H*CH(PR$_3$) and ReCHC*H*(PR$_3$) resonances by comparison with data published previously for mononuclear rhenium ylides [10]. However, similar features were not discerned in the spectrum of [Re$_2$Cl$_3$(μ-dppm)$_2$(CO)(CHCH(PMe$_3$))]PF$_6$ (**3a**) or in that of its PMePh$_2$ analogue **3c**. Instead, the pattern of phenyl resonances integrates for two hydrogens in excess of the number of phenyl ring hydrogens, implying that the ylide hydrogen resonances are buried within these complex patterns. We believe that there may be some fluxional process which involves the ylide ligand of complexes **3a–3c**, the extent of which varies with the nature of the phosphine PR$_3$. Unfortunately, the relatively low solubilities of **3a–3c** make these particular compounds poor candidates for a VT ^{1}H NMR spectral study (see below). One additional point concerns the ^{1}H NMR spectrum of [Re$_2$Cl$_3$(μ-dppm)$_2$(CO)(C(Ph)-CH(PMe$_3$))]PF$_6$ (**3g**) for which two of the resonances associated with the phenyl group of the ylide ligand are found at δ +6.48 (t, 2H) and +5.15 (d, 2H), while the third (expected to be a triplet, 1H) is obscured by the phenyl resonances of the dppm ligand.

The ^{31}P{^{1}H} NMR spectra of all complexes were recorded and found to show very similar features. A singlet for the ylide phosphorus atom was downfield of the two multiplets that characterize the pairs of dppm phosphorus atoms (see Section 2). One of these multiplets is always within the narrow chemical shift range δ −4.0 to −6.5 and is assigned to the pair of P atoms that are bound to the Re that does not have the ylide ligand. The [PF$_6$]$^-$ salts all show a heptet at δ ~ −144 due to the anion. A preliminary VT ^{31}P{^{1}H} NMR study was carried out on a solution of **3d** in (CD$_3$)$_2$CO over the temperature range +35 to −70 °C. Note that the ^{31}P{^{1}H} NMR spectrum of this complex at room temperature in CD$_2$Cl$_2$ (see Section 2) is very similar to that observed in (CD$_3$)$_2$CO. While the singlet at δ +0.74 and the multiplet at δ −4.03 changed very little over this temperature range, the multiplet at δ −16.6 slowly lost its structure, then broadened, and finally collapsed (coalescence temperature ~ −65 °C). Since the latter multiplet is the one we assign to the pair of P atoms that are bound to the Re atom which is also coordinated by the ylide ligand, this supports the occurrence of a fluxional process about the coordinatively unsaturated Re atom; this possibility is also in accord with the interpretation of the ^{1}H NMR spectra of the η^2-ethyne derived complexes **3a–3c** (vide supra).

The NMR spectral properties of the ^{13}C-labeled complex [Re$_2$Cl$_3$(μ-dppm)$_2$(CO)(^{13}CH^{13}CH(PMe$_3$))]-PF$_6$ were not especially informative because of the rather poor solubility properties of this complex. The ^{31}P{^{1}H} spectrum showed broadening of the ylide resonance at δ +6.70, compared to its ^{12}C-labeled analogue **3a**, but no identifiable splitting pattern. The ^{13}C{^{1}H} NMR spectrum showed a broad resonance at δ +96.3 but no other clear-cut signature.

4. Conclusions

The reactions of the η^2-alkyne complexes of dirhenium(II) (**2**) with monodentate tertiary phosphines provide a route to a series of stable ylide complexes **3** (Scheme 1). The scope of this chemistry would seem

[1] A representative example of a non-rhenium containing complex of this type is the manganese species (η^5-C$_5$H$_5$)Mn(CO)$_2$-(C(CO$_2$Me)CH(PPh$_3$)) [9].

to be limited primarily by the range of terminal alkyne complexes of type **2** that can be synthesized. We find no evidence that alkyne dissociation is an important mechanistic step; the products are most likely formed by the direct attack of the PR_3 ligand upon the activated, coordinated terminal alkyne ligand. In contrast, reactions of the mononuclear complexes $Re(O)R_3(PMe_3)$ ($R = Me$ or CH_2SiMe_3) and $Re(O)Me_2Cl(PMe_2R)_2$ with ethyne result in the formal insertion of this alkyne into the Re–P bonds to give the ylides $Re(O)R_3(CHCH(PMe_3))$ and $[Re(O)Me_2(CHCH(PMe_2R))_2]Cl$ [10]. Note that all other alkynes (both terminal and internal) react with $Re(O)Me_3(PMe_3)$ to give the stable η^2-alkyne adducts $Re(O)Me_3(RCCR')$ instead of ylide species [10]. The ylide complexes reported by Hoffman et al. [10] are apparently formed by the loss of PR_3, coordination of ethyne, and subsequent attack of the external (dissociated) phosphine upon the coordinated ethyne. Accordingly, the mechanisms by which our dirhenium ylides and Hoffman's mononuclear rhenium ylide complexes are formed appear to be very similar. However, our dirhenium system has the advantage of being adaptable to a range of different terminal alkynes.

5. Supplementary material

Tables of positional parameters for all non-hydrogen atoms, anisotropic thermal parameters, full listings of bond distances and bond angles, observed and calculated structure factors, and the full atomic numbering scheme for **3i** are available on request from author R.A.W.

Acknowledgement

Support from the National Science Foundation through Grant CHE91-07578 to R.A.W. and a QUEST Fellowship to R.M.T. from NSF-REU Grant CHE92-00343 is gratefully acknowledged.

References

[1] K.-Y. Shih, P.E. Fanwick and R.A. Walton, *Organometallics, 12* (1993) 347.
[2] F.A. Cotton and R.A. Walton, *Multiple Bonds Between Metal Atoms,* Oxford University Press, Oxford, UK, 2nd edn., 1993, Ch. 2.
[3] R.A. Walton, *Polyhedron, 8* (1989) 1689, and refs. therein.
[4] M.E. Woodhouse, F.D Lewis and T.J. Marks, *J. Am. Chem. Soc., 104* (1982) 5586.
[5] N. Walker and D. Stuart, *Acta Crystallogr., Sect. A, 39* (1983) 158.
[6] D.T. Cromer, *International Tables for X-ray Crystallography,* Vol. IV, Kynoch, Birmingham, UK, 1974, (a) Table 2.3.1; (b) Table 2.2B.
[7] J.-S. Qi, P.E. Fanwick and R.A. Walton, *Polyhedron, 9* (1990) 565.
[8] W.J. Geary, *Coord. Chem. Rev., 7* (1971) 81.
[9] N.E. Kolobova, L.L. Ivanov, O.S. Zhvanko, I.N. Chechulina, A.S. Batsanov and Yu.T. Struchkov, *J. Organomet. Chem., 238* (1982) 223.
[10] D.M. Hoffman, J.C. Huffman, D. Lappas and D.A. Wierda, *Organometallics, 12* (1993) 4312.
[11] W.A. Nugent and J.M. Mayer, *Metal–Ligand Multiple Bonds,* Wiley, New York, 1988, p. 190.